J Mater Sci (2007) 42:9194–9199
DOI 10.1007/s10853-007-1919-9

Effects of samarium dopant on photocatalytic activity of TiO_2 nanocrystallite for methylene blue degradation

Qi Xiao · Zhichun Si · Jiang Zhang · Chong Xiao · Zhiming Yu · Guanzhou Qiu

Received: 30 January 2007 / Accepted: 5 June 2007 / Published online: 27 July 2007

Abstract Sm^{3+}-doped TiO_2 nanocrystalline was synthesized by a sol–gel auto-combustion method and characterized by X-ray diffraction, Brunauer-Emmett-Teller method (BET), UV–vis diffuse reflectance spectroscopy (DRS), and also photoluminescence (PL) emission spectroscopy. The photocatalytic activity of Sm^{3+}–TiO_2 catalyst was evaluated by measuring degradation rates of methylene blue (MB) under either UV or visible light. The results showed that doping with the samarium ions significantly enhanced the photocatalytic activity for MB degradation under UV or visible light irradiation. This was ascribed to the fact that a small amount of samarium dopant simultaneously increased MB adsorption capacity and separation efficiency of electron-hole pairs. The results of DRS showed that Sm^{3+}-doped TiO_2 had significant absorption between 400 nm and 500 nm, which increased with the increase of samarium ion content. The adsorption experimental demonstrated that Sm^{3+}–TiO_2 had a higher MB adsorption capacity than undoped TiO_2 and adsorption capacity of MB increased with the increase of samarium ion content. It is found that the stronger the PL intensity, the higher the photocatalytic activity. This could be explained by the points that PL spectra mainly resulted from surface oxygen vacancies and defects during the process of PL, while surface oxygen vacancies and defects could be favorable in capturing the photoinduced electrons during the process of photocatalytic reactions, so that the recombination of photoinduced electrons and holes could be effectively inhibited.

Q. Xiao (✉) · Z. Si · J. Zhang · C. Xiao · G. Qiu
School of Resources Processing and Bioengineering, Central South University, Changsha 410083, China
e-mail: xiaoqi88@mail.csu.edu.cn

Q. Xiao · Z. Yu
School of Materials Science and Engineering, Central South University, Changsha 410083, China

Introduction

Titania is well known as a cheap, nontoxic, efficient photocatalyst for the detoxication of air and water pollutants [1–3]. However, its wide band-gap energy (3.0 eV for rutile and 3.2 eV for anatase) means that only 5% of solar spectrum is used. Moreover, TiO_2 presents a relatively high electron-hole recombination rate, which is detrimental to its photoactivity. In order to solve these problems, several approaches have been proposed, including coupled semiconductor systems [4, 5], noble metals deposition [6], transition metals doping (e.g., Co, Fe) [3, 7], rare earth ions doping (e.g., Nd, La, Ce) [8–11], and nonmetallic elements doping (e.g., N, C, S) [12–14]. Especially, doping with lanthanide ions with 4f electron configurations into TiO_2 lattice could not only eliminate the recombination of electron-hole pairs significantly and but also result in the extension of their wavelength response toward the visible region. Recently, Li et al. [15] reported that the band gap of TiO_2 nanoparticles was reduced by Nd^{3+} doping and the band gap narrowing was primarily attributed to the substitution Nd^{3+} ions which introduced electron states into the band gap of TiO_2 to form the new lowest unoccupied molecular orbital. Xie et al. [16] reported Nd^{3+}–TiO_2 sol catalysts had photocatalytic activity for phenol degradation under visible light irradiation. Li et al. [8] reported that the

introduction of Ce 4f level led to the optical absorption band between 400 nm and 500 nm, and eliminate the recombination of electron-hole pairs and enhance the photocatalytic activity under UV or visible light illumination.

In this study, the photocatalytic activity of Sm^{3+}–TiO_2 catalyst was evaluated by measuring degradation rates of methylene blue (MB) under UV or visible light. The catalyst has been characterized using X-ray diffraction (XRD) technique, photoluminescence (PL), and UV–vis spectrophotometer. The aim of this study was at disclosing the mechanisms of photocatalytic activity enhancement due to samarium ion doping by investigating the effects of samarium ion doping on the contribution of adsorption ability and the separation of electron-hole pairs under either UV or visible light irradiation.

Experimental

Synthesis

Sm^{3+}-doped TiO_2 nanocrystalline was synthesized by a sol–gel auto-combustion method. The detailed process can be described as follows. The analytical grade titanium isopropoxide ($Ti(OC_2H_5)_4$)), $Sm(NO_3)_3$, $C_2H_6O_2$ (ethylene glycol, abbreviated as EG), $C_6H_8O_7$ (citric acid, abbreviated as CA), ammonia (25%) and nitride acid (65–68%) were used as raw materials. Appropriate amount of $Ti(OC_2H_5)_4$) and $Sm(NO_3)_3$ were added to CA and EG mixture under constant stirring condition. The amounts of doped Sm^{3+} are 0.5–1.5 mol%. The molar ratios of CA/Ti and CA/EG were kept constant at 2:1 and 1:1, respectively. After adjusting the pH value with ammonia to 6–7, the mixture solution was evaporated at 90 °C to gradually form a clear precursor gel. The precursor gel was baked at 150 °C in muffle furnace and expanded, then was auto-ignited at about 250 °C. The puffy, porous gray powders as-combusted was calcined at the temperature of 600 °C for 2 h in air. In addition, Degussa P25 TiO_2 (80% anatase, 20% rutile, surface area 35 $m^2\ g^{-1}$) was also employed as photocatalyst in order to compare the photocatalytic activity of the above-mentioned prepared Sm^{3+}-doped TiO_2 nanoparticle with that of Degussa P25 TiO_2.

Characterization

The crystalline structure of the samples was determined by a D/max-γA diffractometer (Cu K_α radiation, λ = 0.154056 nm) studies. The averaged grain sizes D were determined from the XRD pattern according to the Scherrer equation $D = K\lambda/\beta\cos\theta$, where k is a constant (shape factor, about 0.9), λ is the X-ray wavelength (0.15418 nm), β the full width at half maximum (FWHM) of the diffraction line, and θ the diffraction angle. The values of β and θ of anatase and rutile are taken from anatase (101) and rutile (110) diffraction line, respectively. The amount of rutile in the samples was calculated using the following equation [17]: $X_R = (1 + 0.8I_A/I_R)^{-1}$, Where X_R is the mass fraction of rutile in the samples, I_A and I_R are the X-ray integrated intensities of (101) reflection of the anatase and (110) reflection of rutile respectively.

The specific surface area of the powders was measured by the dynamic Brunauer–Emmett–Teller (BET) method, in which a N_2 gas was adsorbed at 77 K using a Micromeritics ASAP 2000 system. The diffuse reflectance spectra (DRS) of the photocatalyst sample in the wavelength range of 200–800 nm were obtained using a UV–vis scanning spectrophotometer (Shimadzu UV-3101) and were converted from reflectance to absorbance by the Kubelka–Munk method. The PL spectra of the samples were recorded with a Fluorescence Spectrophotometer F-4500.

MB adsorption experiment

To determine the adsorption behavior of Sm doped and pure TiO_2 catalyst, we performed a set of adsorption isotherm tests in the dark. In each test, 0.02 g of catalyst was added to 20 mL of MB suspension. The mixture was well dispersed, and put in the dark for 24 h at 298 ± 1 K. The MB concentration in the suspension before and after the adsorption tests was analyzed and the adsorbed amount of MB on the catalysts was calculated based on a mass balance.

Photocatalytic activity

For a typical photocatalytic experiment, 200 mg of the prepared samples TiO_2 nanocrystalline or Degussa P25 TiO_2 was added to 200 mL of the 100 ppm MB aqueous solution. The prepared TiO_2 nanocrystalline samples were dispersed under ultrasonic vibration for 10 min. The solution was kept in the dark under stirring to measure the adsorption of MB into each sample. After keeping at least 20 min, MB concentration in the solution was found to be constant on all samples prepared. Therefore, the solution in which the sample powders were dispersed was kept in the dark for 30 min and then the solution was irradiated under UV or visible light for 120 min duration. For UV irradiation, a 160 W high-pressure mercury lamp fixed at a distance of 150 mm above the surface solution was used as UV light source. The average light intensity was about 600 μW cm^{-2}. The radiant flux was measured with a power

meter from Institute of Electric Light Source (Beijing). For visible light irradiation, a 150 W halogen tungsten lamp with a UV and IR cut-off filter acted as a visible light source to provide light emission at 400–800 nm. The average light intensity was about 3 mW cm^{-2}. After recovering the catalyst by centrifugation, the light absorption of the clear solution was measured at 660 nm (λ_{max} for MB) at a set time. The decolorization of MB was calculated by formula: Decolorization = $(C_0–C)/C_0$, C_0 and C are the concentration of primal and photodecomposed MB. The absorbance of the MB solution was measured with a UV–vis spectrophotometer (Shimadzu UV-3101).

Results

XRD analysis

XRD patterns of Sm^{3+} ions doped titania samples with various samarium content are shown in Fig. 1. From these XRD results, it was shown that the X-ray diffraction peak at 25.5° corresponds to characteristic peak of crystal plane (1 0 1) of anatase, and the peak at 27.6° corresponds to characteristic peak of crystal plane (1 1 0) of rutile. In undoped titania sample, rutile is the dominant crystallized phase, while Sm^{3+}-doped TiO_2 samples shows a mixture phase of anatase and rutile, and the relative ratio of rutile to anatase is reduced with the increase of samarium content. The amount of doped samarium on the crystallite size and rutile content of samarium-doped TiO_2 is shown in Table 1 along with specific surface area. These results show that the presence of samarium result in decrease of both rutile content and crystallite sizes in the samarium doped TiO_2 compared to undoped TiO_2. In addition, it can be also seen that samarium doping content has little influence on crystallite size and rutile content of all the doped samples.

Table 1 The characteristics of Sm^{3+}-doped TiO_2 samples containing different samarium content

Samarium content (%)	Anatase		Rutile		Specific surface area (m^2/g)
	Crystal size $D_{(101)}$ /nm	X_A (%)	Crystal size $D_{(110)}$ /nm	X_R (%)	
0	–	2.41	18.8	97.59	24.52
0.5	13.8	48.39	13.6	51.61	52.75
1.0	12.9	58.22	13.1	41.78	69.48
1.5	12.5	58.33	12.8	41.67	82.94

Diffuse reflectance spectra

To investigate the optical absorption properties of catalysts, we examined the DRS of TiO_2 and Sm^{3+}-doped TiO_2 in the range of 220–850 nm and our results are shown in Fig. 2. It can be seen that while TiO_2 had no absorption in the visible region (>400 nm), Sm^{3+}-doped TiO_2 had significant absorption between 400 nm and 500 nm, which increased with the increase of samarium ion content. In addition, it can be noted that the optical absorption in the UV region was also enhanced. Li et al. [15] reported that the band gap of TiO_2 nanoparticles was reduced by Nd^{3+} doping and the band gap narrowing was primarily attributed to the substitution Nd^{3+} ions which introduced electron states into the band gap of TiO_2 to form the new lowest unoccupied molecular orbital. Further investigation is needed to better understand the reason of the band gap narrowing for Sm^{3+}-doped TiO_2.

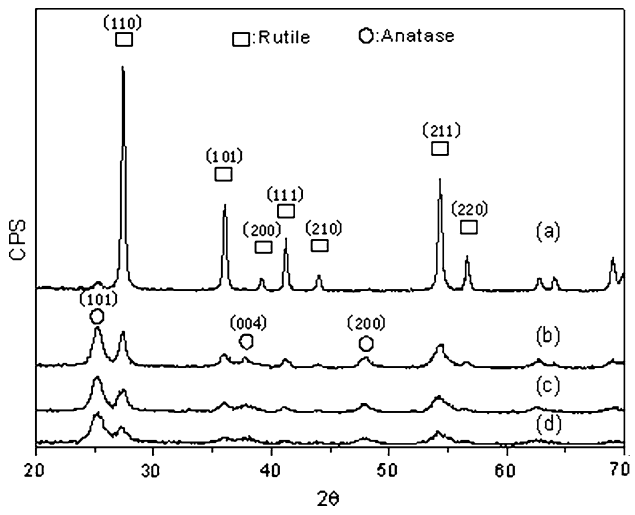

Fig. 1 XRD patterns of TiO_2 with various amounts of samarium (**a**) Undoped; (**b**) 0.5 mol% Sm; (**c**) 1.0 mol% Sm; and (**d**) 1.5 mol% Sm

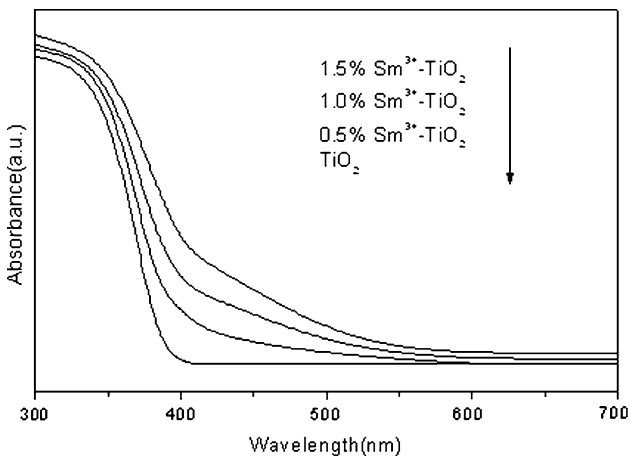

Fig. 2 UV–vis absorption spectra of pure TiO_2 and Sm^{3+}–TiO_2

Fluorescence spectra

The PL emission spectra have been widely used to investigate the efficiency of charge carrier trapping, immigration and transfer, and to understand the fate of electron/hole pairs in semiconductor particles [18]. In this study, Fig. 3 shows the PL spectrum of TiO_2 with various amounts of samarium with the excitation wavelength of 300 nm. It can be seen that the undoped and doped TiO_2 nanoparticles can exhibit obvious excitonic PL signals with similar curve shape, demonstrating that samarium dopant does not give rise to new PL phenomena. TiO_2 nanoparticles could exhibit an obvious PL peaks at about 450 nm with the excited wavelength of 300 nm possibly resulting from bound excitons [19, 20]. There were lots of oxygen vacancies on the surface of TiO_2 nanoparticles, and the size of particle was fine so that the average distance the electrons could move freely was very short. These factors could make the oxygen vacancies very easily bind electrons to form excitons. Thus, the exciton energy level near the bottom of the conduction band came into being, and the PL band of the excitons could also occur. Thus, the stronger the excitonic PL spectrum, the higher the content of surface oxygen vacancy and defect [21]. In addition, the PL intensity gradually increased as samarium content increased, and arrived at the highest degree when samarium content was 0.5 mol%. If samarium contents continued to increase, namely more than 0.5 mol%, the PL intensity began to go down. These results demonstrate that the content of surface oxygen vacancy arrived at the highest degree when samarium content was 0.5 mol%.

Adsorption behavior of methylene blue

The MB adsorption isotherms are shown in Fig. 4. It can be seen that the Sm^{3+}–TiO_2 had a higher MB adsorption capacity than undoped TiO_2. While the saturated adsorption amount of MB onto the TiO_2 was 2×10^{-6} mol g^{-1}, the saturated adsorption amount of MB onto the Sm^{3+}–TiO_2 increased with the increase of samarium ion content up to 9×10^{-6} mol g^{-1}. The factors leading to the enhanced adsorption ability should involve some changes of physical or chemical properties of the catalysts owing to the samarium ion doping. To further study the surface characteristics of the prepared catalysts, we carried out the BET analysis (as shown Table 1). The BET results showed that the specific surface areas of the catalysts increased from 24.52 m^2 g^{-1} for TiO_2 to 82.94 m^2 g^{-1} for 1.5% Sm^{3+}–TiO_2 significantly. The larger specific surface area of Sm^{3+}–TiO_2 catalysts would be beneficial to achieve better physical adsorption of MB in aqueous suspension.

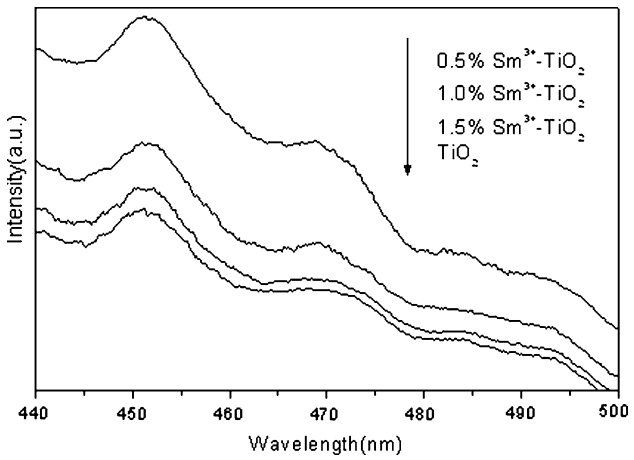

Fig. 3 PL spectrum of samarium doped TiO_2 with the excitation wavelength of 300 nm

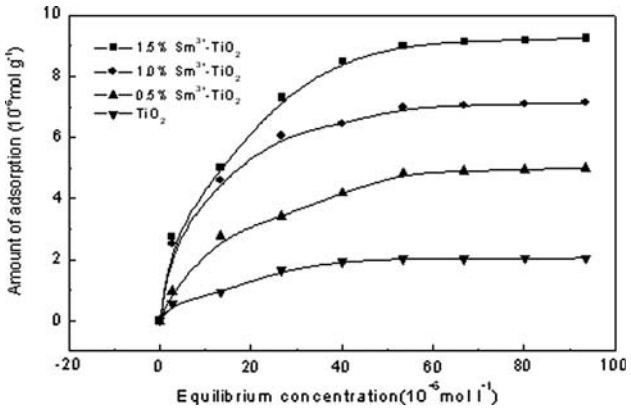

Fig. 4 The MB adsorption isotherms on the pure and doped TiO_2

Photocatalytic activity

The photocatalytic activity of MB over both Sm^{3+}-doped TiO_2 samples and Degussa P25 TiO_2 was evaluated under either UV or visible light and the results are shown in Figs. 5 and 6, respectively. According to Figs. 5 and 6, the photocatalytic activity of the 0.5% Sm^{3+}-doped TiO_2 was higher than that of P25 both under UV and vis light. These results indicate that Sm^{3+}-doped TiO_2 is potentially employable for photodegradation processes under UV or vis light. It also was found that the order of photocatalytic activity of samarium doped TiO_2 nanoparticles at 120 min was as following: 0.5 > 1.0 > 1.5 > 0 mol%, which suggests that the Sm^{3+} doping enhances the photocatalytic activity of TiO_2 and there is an optimum doping content of Sm^{3+} ions in TiO_2 particles. In addition, the XRD results show that the undoped titanium dioxide was almost rutile, while the rest of Sm^{3+} doping samples had approximately 50% anatase. Recently, it has been found that a mixture of anatase and rutile TiO_2 nanoparticles has

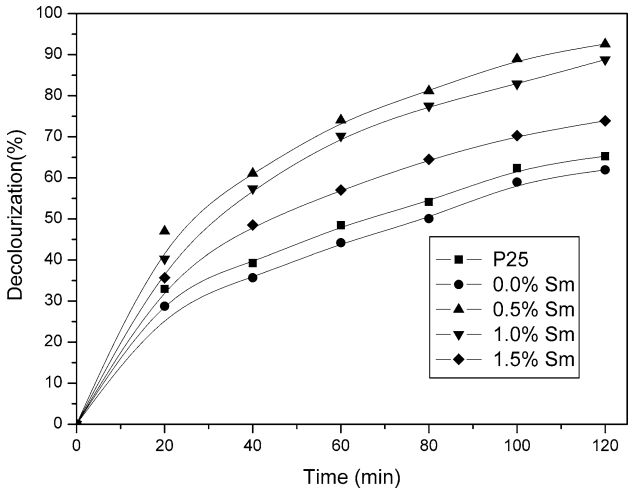

Fig. 5 Photocatalytic decomposition profiles of MB Over different samarium doped TiO_2 and P25 under UV irradiation

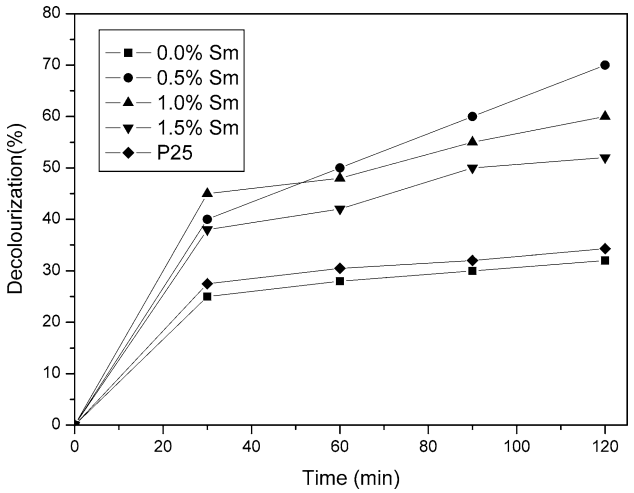

Fig. 6 Photocatalytic decomposition profiles of MB Over different samarium doped TiO_2 and P25 under visible irradiation

a much higher photocatalytic activity than pure anatase or pure rutile TiO_2 nanoparticles under UV light excitation [22]. The remarkable coexistent effect of rutile and anatase would arise from the increase in the charge separation efficiency due to photo-induced interfacial electron transfer from anatase to rutile under UV light excitation [23]. According to Figs. 5 and 6, it is clear that the photocatalytic activity is drastically increased under the presence of a small amount of anatase phase (only 5.9% anatase) compared to pure rutile and the sample calcined at 600 °C consists of mixed phases with approximately 50% anatase shows the highest photocatalytic activity. These results strongly suggest the existence of a synergistic effect between anatase and rutile powders in the Sm^{3+}-doped TiO_2 under Vis light excitation, which is siminar to that of TiO_2 under UV light excitation [22, 23].

In addition, the reason that there is an optimum doping content of Sm^{3+} ions in TiO_2 particles should be further understood. Some studies indicated that the photocatalytic activity of TiO_2 catalysts depends strongly on two factors: adsorption behavior and the separation efficiency of electron-hole pairs [1, 24, 25].

The photoinduced electron transfer to adsorbed organic species results from migration of electrons and holes to the semiconductor surface. The electron transfer process is more efficient if the species are preadsorbed on the surface [26]. According to Figs. 4 and 5 or Fig. 6, the photocatalytic reactivity of Sm^{3+}–TiO_2 is higher than that of undoped TiO_2, which is consistent with the higher adsorption capacity of Sm^{3+}–TiO_2 than undoped TiO_2. However, it was noticeable that a higher adsorption capacity with a higher samarium ion dosage did not lead to a higher photocatalytic activity, which might be limited by lower separation efficiency of electron-hole pairs.

According to Figs. 3 and 5 or Fig. 6, it can be found that the order of photocatalytic activity was the same as that of PL intensity, namely, the stronger the PL intensity, the higher the photocatalytic activity. During the process of PL, oxygen vacancies and defects could bind photoinduced electrons to form free or binding exactions so that PL signal could easily occur, and the larger the content of oxygen vacancies or defects, the stronger the PL intensity [21]. But, during the process of photocatalytic reactions, oxygen vacancies and defects could become the centers to capture photoinduced electrons so that the recombination of photoinduced electrons and holes could be effectively inhibited. Moreover, oxygen vacancies could promote the adsorption of O_2, and there was strong interaction between the photoinduced electrons bound by oxygen vacancies and adsorbed O_2. This indicated that the binding of photoinduced electrons on oxygen vacancies could make for the capture for photoinduced electrons of adsorbed O_2, and·O_2 free group was produced at the same time. Thus, oxygen vacancies and defects were in favor of photocatalytic reactions in that O_2 was active to promote the oxidation of organic substances [1, 27]. The above results demonstrated that there were certain relationships between PL spectra and photocatalytic activity, namely, the stronger the PL intensity, the larger the content of oxygen vacancies and defects, the higher the photocatalytic activity. Therefore, in this study 0.5 mol% may be the most suitable content of Sm^{3+} in the Titania, at which the recombination of photoinduced electrons and holes could be effectively inhibited and thereby the highest photocatalytic activity is formed.

Conclusion

Doping with the samarium ions significantly enhanced the overall photocatalytic activity for MB degradation under UV or visible light irradiation. Sm dopant had a great inhibition on TiO_2 phase transformation, and gave rise to significant absorption band between 400 nm and 500 nm, which increased with the increase of samarium ion content. Sm^{3+}–TiO_2 had a higher MB adsorption capacity than undoped TiO_2. It is found that the stronger the PL intensity, the larger the content of oxygen vacancies and defects, the higher the photocatalytic activity. Therefore, in this study 0.5 mol% may be the most suitable content of Sm^{3+} in the Titania, at which the recombination of photoinduced electrons and holes could be effectively inhibited and thereby the highest photocatalytic activity is formed.

Acknowledgments This work was supported by the Provincial Excellent PhD Thesis Research Program of Hunan (No.2004-141) and the Postgraduate Educational Innovation Engineering of Central South University (No.2006-48). The authors are grateful to Dr. Huang Suping for her encouragement and helpful discussion.

References

1. Hoffmann MR, Choi ST, Martin W, Bahnemann DW (1995) Chem Rev 95:69
2. Fujishima A, Rao TN, Truk DA (2000) J Photochem Photobiol C: Photochem Rev 1:1
3. Choi W, Termin A, Hoffmann MR (1994) J Phys Chem 98:13669
4. Hattori A, Tokihisa Y et al (2000) J Electrochem Soc 147:2279
5. Wang C, Xu B-Q (2005) J Solid State Chem 178:3500
6. Iliev V, Tomova D et al (2006) Appl Catal B: Environ 63:266
7. Kim DH, Woo SI et al (2005) Solid State Commun 136:554
8. Li FB, Li XZ, Hou MF, Cheah KW, Choy WCH (2005) Appl Catal A: Gen 285:181
9. Zhang Y, Xu H, Xu Y, Zhang H, Wang Y (2005) J Photochem Photobiol A: Chem 170:279
10. Yan X, He J, Evans DG, Duan X, Zhu Y (2005) Appl Catal B: Environ 55:243
11. Xie Y, Yuan C, Li X (2005) Mater Sci Eng B 117:325
12. Asahi R, Morikawa T, Ohwaki T, Aoki K, Taga Y (2001) Science 293:269
13. Kamisaka H, Adachi T, Yamashita K (2005) J Chem Phys 123:084704
14. Madhusudan Reddy K, Baruwati B, Jayalakshmi M, Mohan Rao M, Manorama SV (2005) J Solid Chem 178:3352
15. Li W, Wang Y, Lin H, Ismat Shah S, Doren CP, Rykov SA, Chen JG, Barteau MA (2003) Appl Phys Lett 83:4143
16. Xie YB, Yuan CW (2004) Appl Surf Sci 221:17
17. Spurr RA, Myers H (1957) Anal Chem 29:760
18. Yamashita H, Ichihashi Y, Zhang SG, Matrumura Y, Souma Y, Tatsumi T, Anpo M (1997) Appl Surf Sci 121/122:305
19. Zhang LD, Mo CM (1995) Nanostruct Mater 6:831
20. Danzhen L, Yi Z, Xianzhi F (2000) Chin J Mater Res 14:639
21. Jing L, Xin B, Yuan F, Xue L, Wang B, Fu H (2006) J Phys Chem B 110:17860
22. Hurum DC, Agrios AG, Gray KA, Rajh T, Thurnauer MC (2003) J Phys Chem B 107:4545
23. Miyagi T, Kamei M, Mitsuhashi T, Ishigaki T, Yamazaki A (2004) Chem Phys Lett 390:399
24. Fujishima A, Rao TN, Tryk DA (2000) J Photochem Photobiol C: Photochem Rev 1:1
25. Kamat PV (1993) Chem Rev 93:267
26. Linsebigler AL, Lu G, Yates JT (1995) Chem Rev 95:735
27. Liu H, Cheng S, Wu M, Wu H, Zhang J, Li W, Cao C (2000) J Phys Chem A 104:7016